Neuron

Supplemental Information

Local and Distant Input Controlling Excitation in Layer II of the Medial Entorhinal Cortex

Elke C. Fuchs, Angela Neitz, Roberta Pinna, Sarah Melzer, Antonio Caputi, and Hannah Monyer

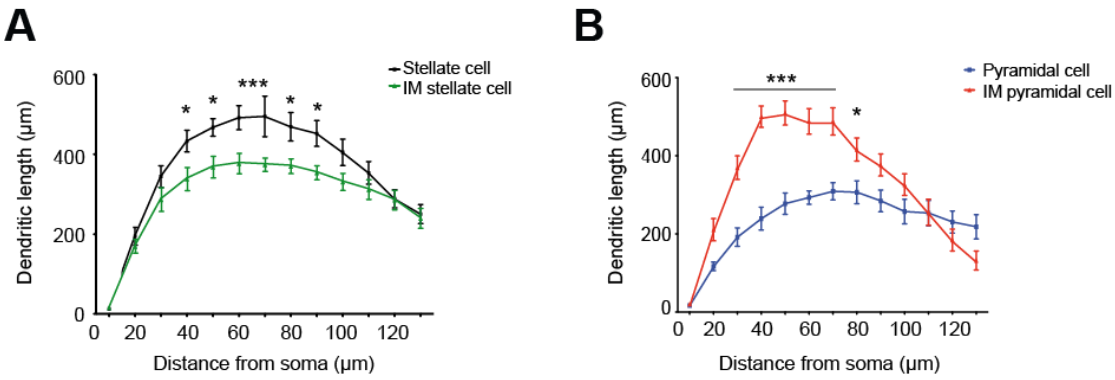

Figure S1. Sholl analysis of dendrites reconstructed from biocytin-filled LII excitatory cells, related to Figure 1

(A) The dendritic density of stellate cells was significantly higher at short distances (40-90 μm) from the soma when compared to that of intermediate stellate cells.

(B) The dendritic density of pyramidal cells was significantly lower at short distances (30-80 μm) from the soma when compared to that of intermediate pyramidal cells (*$p < 0.05$; ***$p < 0.001$, two-way ANOVA followed by post-hoc Bonferroni test). Data represent mean ± SEM. Abbreviations: IM, intermediate.

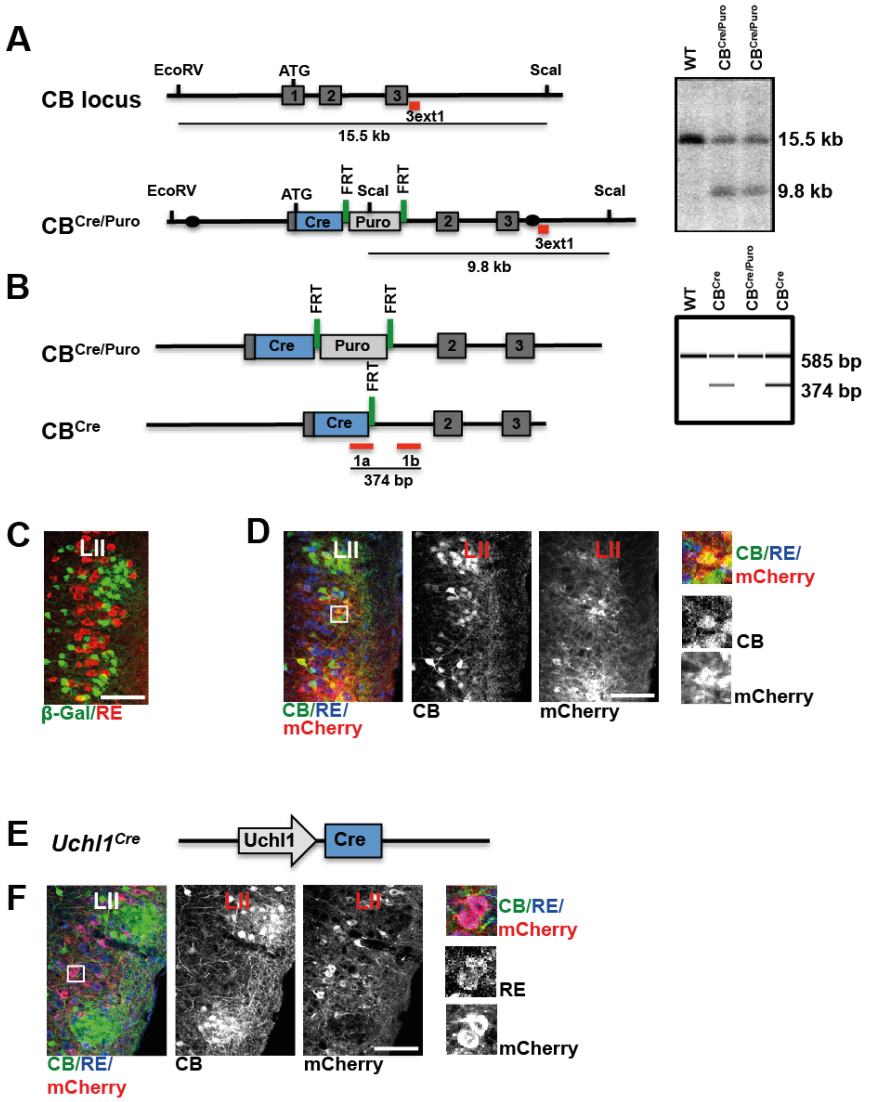

Figure S2. *CB*^{Cre} and *Uchl1*^{Cre} mouse lines used to fluorescently label CB^{+} and RE^{+} neurons in LII, related to Figure 2

(A) Generation of the *CB*^{Cre} mouse via knock-in approach. Schematic representation of gene segments of the wild-type (WT) CB allele and the targeted CB$^{Cre/Puro}$ allele. Dark grey boxes indicate exons, blue box represent Cre recombinase and solid circles indicate the 5' and 3' end of the targeting vector. Positions for EcoRV and ScaI restricition sites are indicated. The green bars stand for the FRT sites flanking the puromycin selection cassette

(Puro). The location of the PCR fragment used as probe for Southern blot analysis is shown as a red bar (left). Southern blot analysis of genomic DNA obtained from WT and $CB^{Cre/Puro}$ ES cells with the 3' external probe demonstrating the presence of a 9.8 kb fragment specific for the modified allele (the 15.5 kb fragment derives from the WT allele; right).

(B) Removal of the puromycin selection cassette after breeding of $CB^{Cre/Puro}$ with FLP deleter mice. The locations of the primer (1a and 1b) used for the demonstration for the removal of puromycin selection cassette are shown as red bars (left). PCR analysis of genomic DNA from WT, $CB^{Cre/Puro}$ and CB^{Cre} mice. The 585 bp control band indicates the presence of genomic DNA and the 374 pb fragment demonstrates the successful removal of the puromycin selection cassette in DNA obtained from CB^{Cre} mice (right).

(C) Crossing CB^{Cre} mice with *ROSA26* reporter mice revealed cell type-specific expression of the reporter gene β-galactosidase in RE^- LII neurons (97 ± 0.6% of β-galactosidase$^+$ neurons were RE^-; 2211 RE^+ and 1434 β-galactosidase$^+$ cells analyzed in 3 CB^{Cre} *x ROSA26* mice).

(D) Confocal picture of immunostaining against CB and RE in LII following AAV DIO ChR2-mCherry injection into the MEC of a CB^{Cre} mouse (left panel). CB staining and mCherry expression of the same section (middle panels). Boxed double-labeled neurons are shown on the right as merged image and the single channels for CB and mCherry. Scale bar, 100 μm.

(E) Schematic drawing showing the transgenic construct used to generate the $Uchl1^{Cre}$ mouse line. Gray arrow represents the *Uchl1* promoter and blue box indicates Cre recombinase.

(F) Confocal picture of immunostaining against CB and RE in LII following AAV DIO ChR2-mCherry injection into the MEC of an *Uchl1*^{Cre} mouse. CB staining and mCherry expression of the same section (middle panels). Boxed double-labeled neurons are shown on the right as merged image and the single channels for RE and mCherry. Scale bar, 100 μm.

Cre recombinase expression in *Uchl1*^{Cre} was restricted to RE^{+} neurons in LII (93.2 ± 2.6% of mCherry^{+} neurons expressed RE; 597 mCherry^{+} and 1272 RE^{+} neurons analyzed in 3 hemispheres from 3 AAV DIO ChR2-mCherry-injected *Uchl1*^{Cre} mice).

Abbrevations: CB, calbindin; Cre, Cre recombinase; β-Gal, β-galactosidase; L, layer; WT, wild-type; Puro, puromycin selection cassette; RE, reelin.

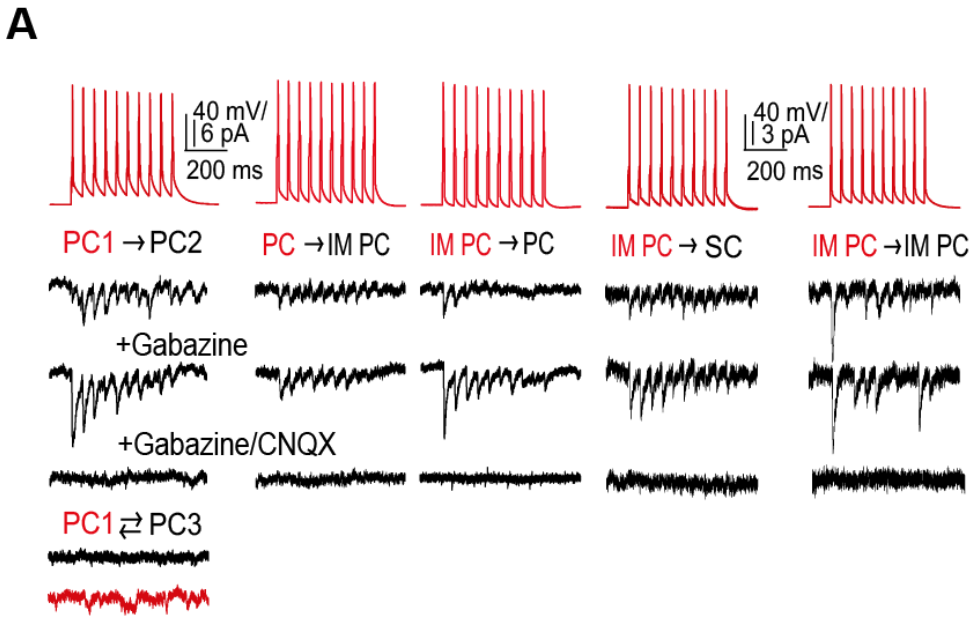
A
40 mV/
6 pA
200 ms
40 mV/
3 pA
200 ms
PC1 → PC2
PC → IM PC
IM PC → PC
IM PC → SC
IM PC → IM PC
+Gabazine
+Gabazine/CNQX
PC1 ⇄ PC3

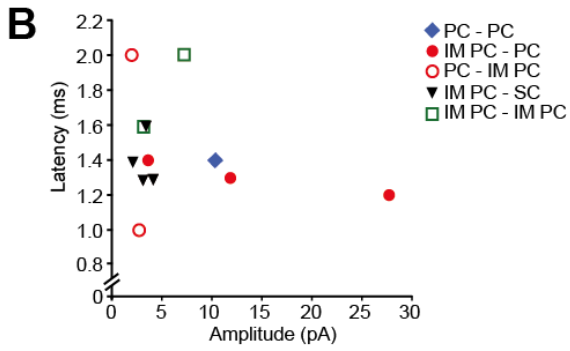
B
PC - PC
IM PC - PC
PC - IM PC
IM PC - SC
IM PC - IM PC
Latency (ms)
Amplitude (pA)

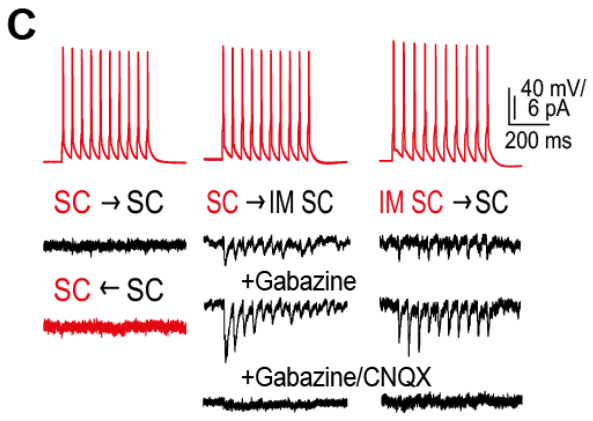
C
40 mV/
6 pA
200 ms
SC → SC
SC → IM SC
IM SC → SC
SC ← SC
+Gabazine
+Gabazine/CNQX

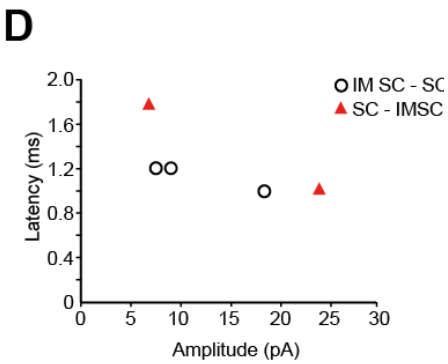
D
IM SC - SC
SC - IMSC
Latency (ms)
Amplitude (pA)

Figure S3. Excitatory connectivity in MEC LII of *CB*^{Cre} and *Uchl1*^{Cre} mice, related to Figure 2

(A) Magnified traces of excitatory cell pairs recorded in *CB*^{Cre} mice, shown in **Figure 2B**, including the single connected PC-PC pair (not shown in **Figure 2;** the neuron termed PC1 was the same presynaptic neuron both for PC2 and PC3). Unitary EPSCs were tested pharmacologically for their excitatory nature. Gabazine and CNQX (both 10 μM), sequentially, but not Gabazine alone, blocked uEPSCs effectively.

(B) Graph depicting averaged peak amplitudes and latencies of the first uEPSCs of all connected LII cell pairs recorded in *CB*^{Cre} mice.

(C) Magnified traces of SC-SC and IM SC-SC cell pairs recorded in *Uchl1*^{Cre} mice, shown in **Figure 2D.**

(D) Graph representing peak amplitudes and latencies of uEPSCs of all connected IM SC-SC cell pairs recorded in *Uchl1*^{Cre} mice.

Abbreviations: PC, pyramidal cell; SC, stellate cell; IM PC, intermediate pyramidal cell; IM SC intermediate stellate cell.

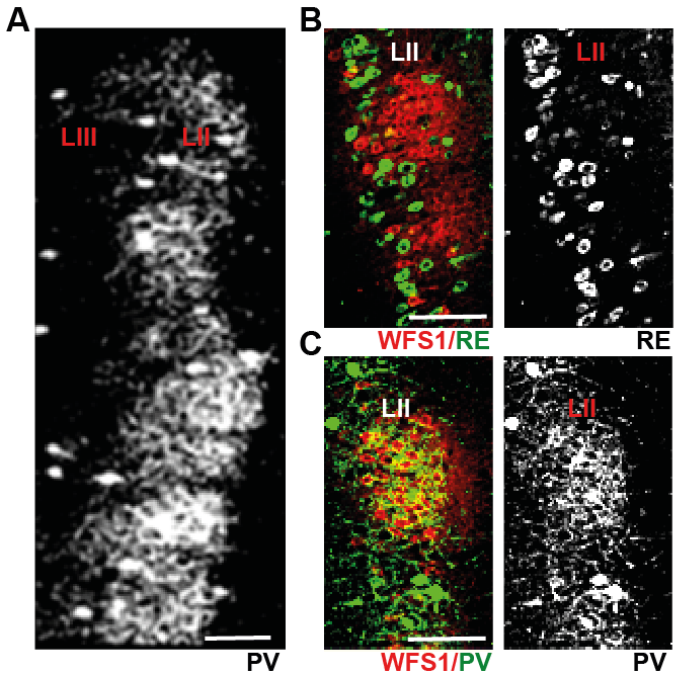

Figure S4. Modular organization of PV$^+$ axons in LII of the MEC, related to Figure 3

(A) PV immunoreactivity in LII of the MEC (sagittal section).

(B) Double-labeling for WFS1 and RE in LII (left), single channel for RE (right).

(C) Double-labeling for WFS1 and PV in LII (left), single channel for PV (right).

Scale bars, 100 μm. Abbreviations: L, layer; PV, parvalbumin; RE, reelin.

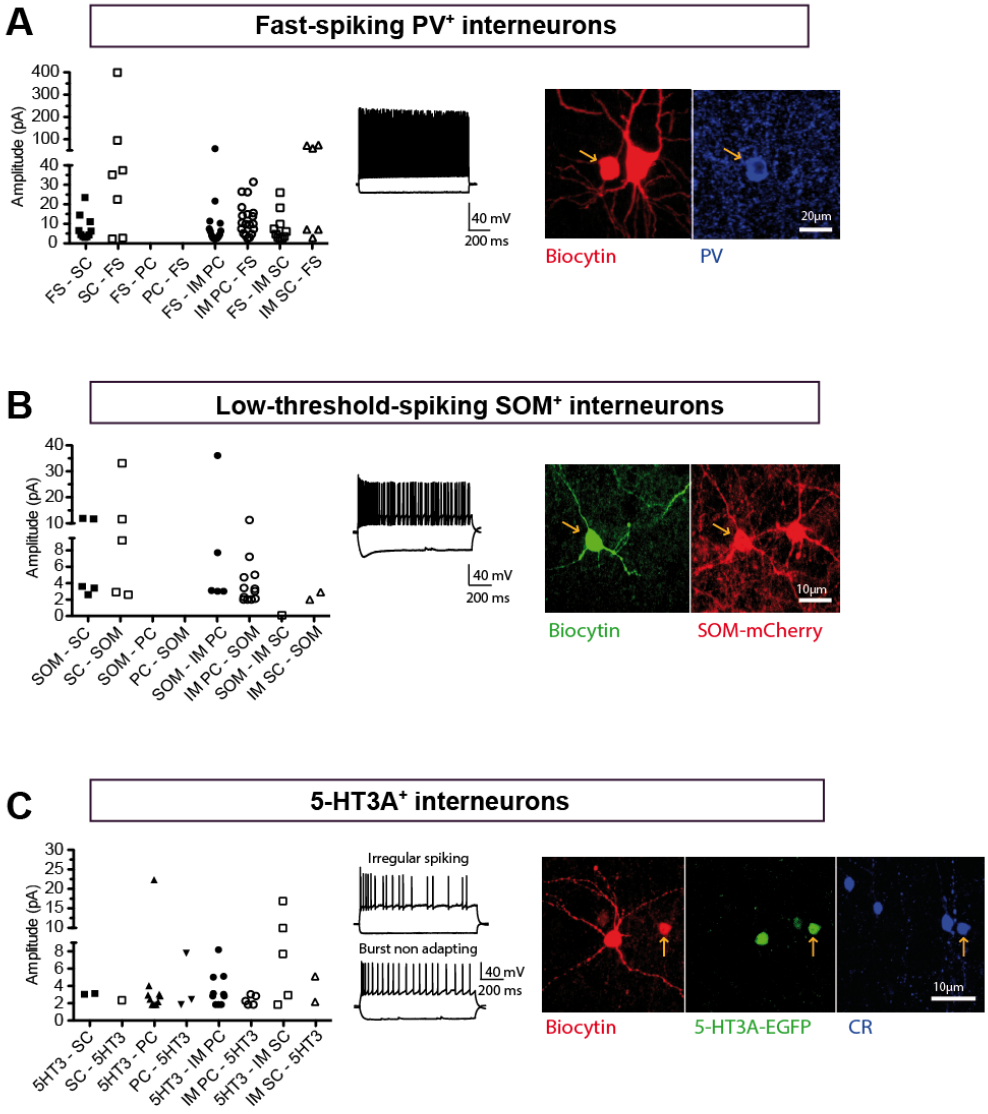

Figure S5. Inhibitory connectivity in MEC LII, related to Figure 3

(A) Graph on the left side represents peak amplitudes of uIPSC and uEPSCs recorded from pairs of FS interneurons and indicated excitatory cells. FS interneurons exhibited a non-adapting spike firing at > 80 Hz, as illustrated in the middle panel, and expressed the Ca^{2+}-binding protein PV (indicated by the yellow arrow in the right panel).

(B) Graph depicting peak amplitudes of uIPSCs and uEPSCs recorded in

pairs of SOM^+ interneurons and indicated excitatory cells. SOM^+ interneurons are characterized by a prominent hyperpolarizing sag, low-threshold firing and spike adaptation, as shown in the middle panel. SOM^+ interneurons in MEC LII of *SOM*^{Cre} mice are labeled with biocytin (green) and express mCherry (red, right panel).

(C) Graph illustrates peak amplitudes of uIPSCs and uEPSCs in pairs of 5-HT_{3A}^{EGFP+} interneurons and indicated excitatory cells. The 5-HT_{3A}^+ interneuron population is a diverse group, including irregular spiking cells (upper middle panel) and burst, non-adapting cells (lower middle panel). Some 5-HT_{3A}^+ interneurons expressed CR (blue; indicated by the yellow arrow in the right panel).

Abbreviations: PC, pyramidal cell; SC, stellate cell; IM PC, intermediate pyramidal cell; IM SC intermediate stellate cell; CR, calretinin; EGFP, enhanced green fluorescent protein; 5-HT_{3A}, 5-HT_{3A} receptor; SOM, somatostatin.

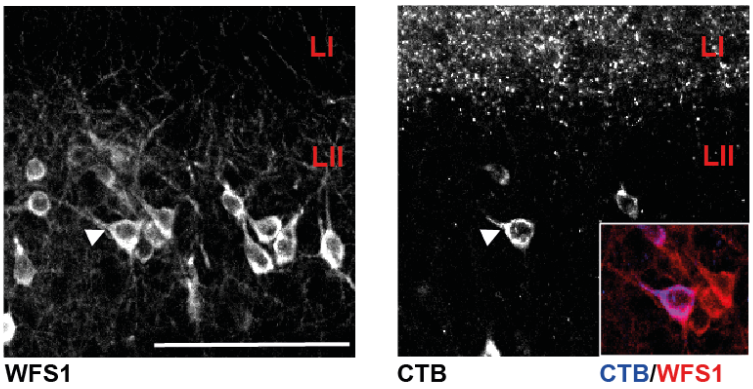

Figure S6. Contralaterally projecting WFS1$^+$ LII neurons, related to Figure 4

Oblique orientation of the main apical dendrite (indicated by white arrowhead) of a WFS1$^+$ (left) and CTB$^+$ (right) neuron in LII. Inset is a higher magnification of the WFS1$^+$/ CTB$^+$ neuron. Scale bar, 100 µm. Abbrevations: L, layer; CTB, Cholera Toxin subunit B.

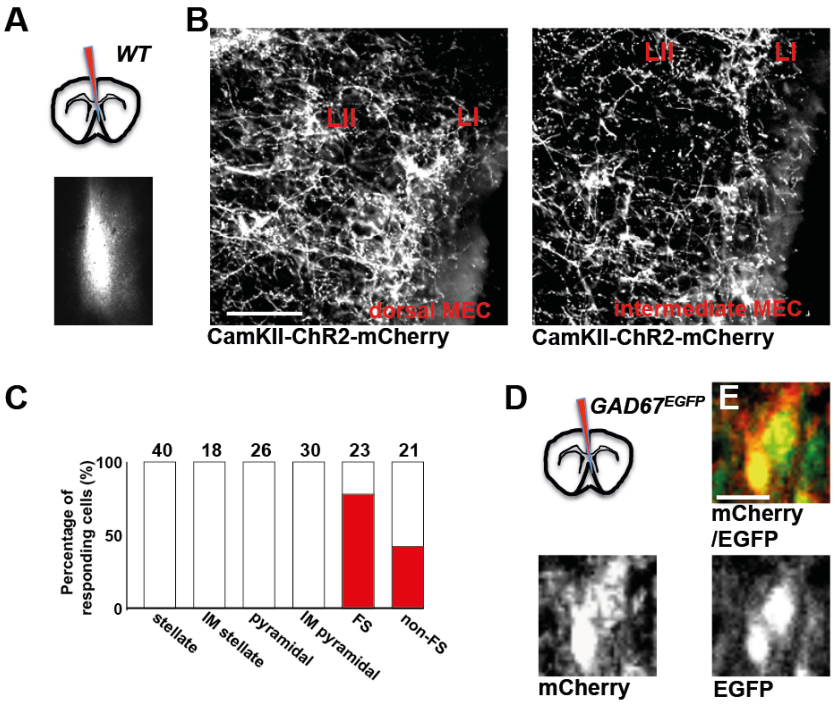

Figure S7. Identification of LII target cells after injection of AAV CamKII ChR2-mCherry into the MS of WT mice, related to Figure 7

(A) Schematic drawing indicating the site of virus injection in the MS (upper panel). MCherry expression following AAV CamKII ChR2-mCherry injection into the MS of a WT mouse (coronal section; lower panel).

(B) ChR2-mCherry^{+} axons in LII of the dorsal (left panel) and intermediate (right panel) MEC (sagittal sections). Scale bar, 50 µm.

(C) Histogram indicating percentage of responding neurons in LII following optogenetic stimulation. Responses could be detected only in FS and non-FS interneurons (red) and were all inhibitory as indicated by the GABAergic reversal potential and the pharmacological blockage with Gabazine, but not with D-AP5 and CNQX (data not shown). Numbers indicate the total number of analyzed neurons (from 16 mice).

(D) Schematic drawing indicating the site of AAV CamKII ChR2-mCherry injection into the MS of a *GAD67*^{EGFP} mouse.

(E) AAV CamKII ChR2-mCherry injection into the MS of *GAD67*^{EGFP} mice demonstrated that expression was not confined to glutamatergic cells, but was also expressed in GABAergic neurons. Co-labeling of mCherry and EGFP (upper panel), single channel for mCherry and EGFP shown in the two lower panels. Scale bar, 10 μm.

Abbreviations: L, layer; ChR2, channelrhodopsin; EGFP, enhanced green fluorescent protein; FS, fast-spiking interneuron; non-FS, non fast-spiking interneuron; IM, intermediate; MEC, medial entorhinal cortex.

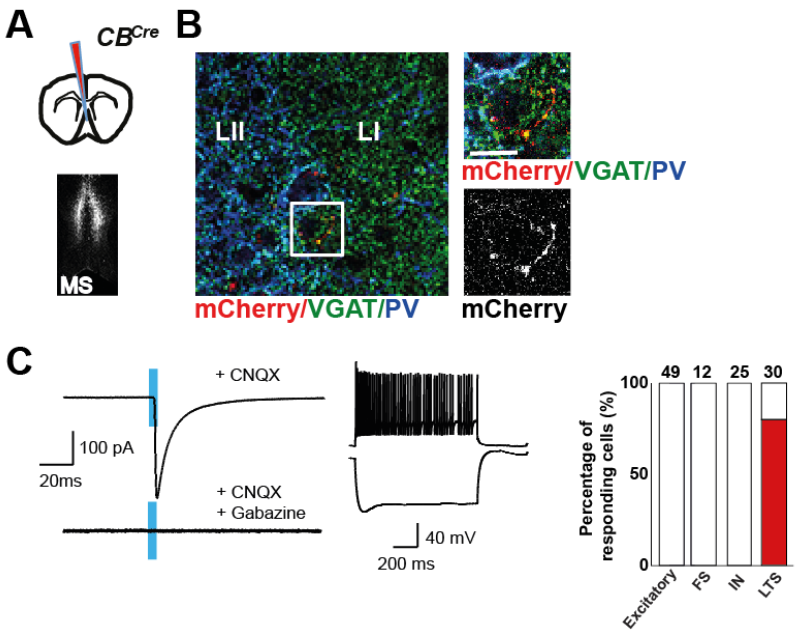

Figure S8. Identification of LII target cells after injection of AAV DIO ChR2-mCherry into the MS of *CB*^{Cre} mice, related to Figure 7

(A) Schematic drawing indicating the site of virus injection in the MS (upper panel). MCherry expression following AAV DIO ChR2-mCherry injection into the MS of a *CB*^{Cre} mouse (coronal section; lower panel).

(B) ChR2-mCherry^{+} axons colocalized with VGAT in the transition zone between LI and LII of the dorsal MEC (sagittal sections). Boxed double-labeled mCherry^{+} axon is shown right (single channel for mCherry in the lower panel). Scale bar, 10 µm.

(C) Synaptic responses and firing pattern of a targeted LTS interneuron, ChR2-mCherry-expressing axons were stimulated by 5 ms laser pulses (blue bar) and IPSCs were recorded. The inhibitory input was identified in the presence of the indicated antagonists. Histogram represents percentage of responding neurons in LII following optogenetic stimulation. Responses were detected only in LTS interneurons (red). IN stands for interneurons, which had

a firing pattern different from FS or LTS interneurons. Total number of analyzed neurons (from 9 mice) is indicated above the bars.

Abbreviations: L, layer; ChR2, channelrhodopsin; CB, calbindin; FS, fast-spiking interneuron; IN, interneuron; LTS, low-threshold-spiking interneuron; MS, medial septum, PV, parvalbumin; VGAT, vesicular GABA transporter.

Cell type	Stellate cells	Pyramidal cells	Intermediate stellate cells	Intermediate pyramidal cells
WFS1/ RE	100 % RE^+ (n = 51 cells)	89.7% $WFS1^+$ 7.6% RE^+ 2.5% $WFS1^+/RE^+$ (n = 39 cells)	73.9% RE^+ 26.1% $WFS1^+/RE^+$ 0% $WFS1^+$ (n = 26 cells)	55.2% $WFS1^+$ 37.9% $WFS1^+/RE^+$ 10.3% RE^+ (n = 36 cells)
V_{rest} (mV)	-65.38 ± 0.33 (#)	-69.98 ± 0.62 (*)	-64.75 ± 0.52 (#)	-67.66 ± 1.20 (#,*)
R_{in} (M**Ω**)	40.73 ± 0.86 (#)	54.02 ± 1.13 (*)	47.72 ± 1.29 (#)	53.08 ± 1.26 (#,*)
sag (mV)	3.73 ± 0.12 (#)	0.11 ± 0.02 (*)	3.77 ± 0.30 (#)	2.06 ± 0.13 (#,*)
Rebound depolarization (mV)	4.52 ± 0.14 (#)	0.56 ± 0.08 (*)	4.22 ± 0.23 (#)	2.52 ± 0.15 (#,*)
latency to spike firing (ms)	23.85 ± 0.70 (#)	206.96 ± 13.74 (*)	350.95 ± 32.55 (#,*)	246.61 ± 22.86 (#,*)
Spike threshold (mV)	-42.23 ± 0.31 (#)	-41.06 ± 0.37 (*)	-42.48 ± 0.48 (*)	-40.75 ± 0.56 (*)
Spike halfwidth (ms)	0.85 ± 0.02 (#)	0.97 ± 0.02 (*)	0.84 ± 0.02 (#)	0.86 ± 0.02 (#)
fAHP (mV)	4.08 ± 0.24	3.83 ± 0.25	5.54 ± 0.31 (#,*)	6.99 ± 0.27 (#,*)
dAP (mV)	2.35 ± 0.09 (#)	0.04 ± 0.008 (*)	1.46 ± 0.11 (#,*)	1.56 ± 0.05 (#,*)
mAHP (mV)	8.39 ± 0.26	9.20 ± 0.26	8.55 ± 0.40	8.90 ± 0.23
ratio of ISI1/ISI2	0.04 ± 0.002 (#)	0.80 ± 0.01 (*)	0.07 ± 0.003 (#,*)	0.70 ± 0.02 (*)

Table S1. Electrophysiological properties of indicated excitatory cells in MEC layer II, related to Figure 1

Characterization of excitatory cell types in MEC layer II of wild type mice, consisting of: (I) stellate cells (n = 128 cells), (II) pyramidal cells (n = 138 cells), (III) intermediate stellate cells (n = 63 cells) and (IV) intermediate pyramidal cells (n = 116 cells). Characteristic electrophysiological properties were analyzed and biocytin-filled cells tested for WFS1- and RE-expression. N equals number of immunostained cells. Abbreviations: RE, reelin; V_{rest}, resting membrane potential; R_{in}, input resistance; fAHP, fast after hyperpolarization amplitude; mAHP, medium after hyperpolarization amplitude; dAP, depolarizing afterpotential; ISI, interspike interval. Data represent mean ± SEM; $p < 0.05$; * significantly different compared to stellate cells; # significantly different compared to pyramidal cells using one-way ANOVA followed by post-hoc Fischer LSD test.

Cell type	Stellate	Intermediate stellate	Intermediate pyramidal	Pyramidal	FS	non-FS
Percentage of responding cells	56 % (n=34)	64 % (n=28)	36 % (n=60)	35 % (n=31)	70 % (n=20)	10 % (n=20)
Number of monosynaptically responding cells	4 (n=13)	1 (n=17)	0 (n=15)	0 (n=8)	1 (n=10)	0 (n=2)
Number of monosynaptic responses blocked by D-AP5/CNQX	4 (n=4)	1 (n=1)	n.d.	n.d.	1 (n=1)	n.d.
Amplitude of monosynaptic response (pA)	14.93 ± 1.77 (n=4)	20.89 (n=1)	n.d.	n.d.	6.12 (n=1)	n.d.
Latency of monosynaptic response (ms)	2.61 ± 0.05 (n=4)	3.89 (n=1)	n.d.	n.d.	3.54 (n=1)	n.d.

Table S2. Responses of LII target cells receiving excitatory input from contralateral CB$^+$ neurons, related to Figure 4

N equals number of recorded cells. Data represent mean ± SEM. Abbreviations: FS, fast-spiking interneuron; non-FS, non fast-spiking interneuron; n.d., not detected.

Supplemental Experimental Procedures

Animals

We used wild-type C57Bl/6, *GAD67*^{EGFP} (Tamamaki et al., 2003), *CB*^{Cre} (purchased from Taconic Biosciences, Cologne, Germany), *Uchl1*^{Cre} (obtained from Mutant Mouse Regional Resource Center, USA), *PV*^{Cre} (Hippenmeyer et al., 2005), *SOM*^{Cre} (Melzer et al., 2012) and *5HT*$_{3A}$^{EGFP} (Inta et al., 2008) mice. All procedures involving wild-type, and genetical modified mice had ethical approval from the Regierungspräsidium Karlsruhe, Germany (AZ 35-9185.81/ G-173-12) and (G-254-14).

Uchl1^{Cre} mice

The mouse strain used for this research project, STOCK Tg(Uchl1-cre)NO63Gsat/Mmucd, identification number 036089-UCD, was obtained from the Mutant Mouse Regional Resource Center, a NCRR-NIH funded strain repository, and was donated to the MMRRC by the NINDS funded GENSAT BAC transgenic project.

Retrograde tracer injection

Eight weeks old male wild-type and *GAD67*^{EGFP} mice were injected with 100 nl Cholera Toxin subunit B (Alexa Fluor 488 Conjugate or Alexa Fluor 555 Conjugate, Life Technology GmbH, Germany), or injected with 70 nl Fluorogold (0.5%, Fluorochrome, Denver, USA). Animals were anesthetized with isoflurane, mounted in a stereotactic apparatus and kept under isoflurane anesthesia during surgery.

For medial entorhinal cortex (MEC) injections, coordinates were 3.1 mm lateral from the midline, 0.1 mm anterior to the transverse sinus and 1.8 mm below the cortical surface. The glass micropipette with a tip resistance of 2 to 4 MΩ was lowered into the cortex with an antero-posterior angle of 6°. The pipette was held in place for 20 min before being retracted from the brain.

For dorsal hippocampal injections a small craniotomy was made 2.4 mm posterior to bregma and 2.0 mm lateral to the midline. Retrograde tracer was delivered through a small durotomy by a glass micropipette with a tip resistance of 2 to 4 MΩ, 1.6 mm below the cortical surface into the dorsal hippocampus.

For medial septum (MS) injections a small craniotomy was made 1 mm anterior to bregma. Retrograde tracer was delivered by a glass micropipette with a tip resistance of 2 to 4 MΩ, 4 mm below the cortical surface into the medial septum.

The scalp incision was sutured, and post-surgery analgesics were given to aid recovery (0.03 mg/kg KG Metamizol). Animals were perfused 5 to 12 days after injection and the brains processed with immunohistochemical methods.

We did not analyze mice in which the injection site did not correspond to the aimed area.

Virus Injections

pAAV-double floxed-hChR2(H134R)-mCherry-WPRE-pA (AAV DIO ChR2-mCherry) vector was obtained from Karl Deisseroth (Cardin et al., 2010). This vector carries an inverted version of Channelrhodopsin 2 fused to the fluorescent marker mCherry. In the presence of Cre recombinase, the

cassette is inverted into the sense direction and the fused proteins are expressed from the EF1 promoter. AAV chimeric vectors (virions containing a 1:1 ratio of AAV1 and AAV2 capsid proteins with AAV2 ITRs) were generated as described (Klugmann et al., 2005). AAV CaMKIIa.hChR2(h134a)-mCherry virus was obtained from Pennvector Core (Penn University, USA).

We injected 8 weeks old male and female *CB^{Cre}*, *Uchl1^{Cre}, PV^{Cre} and SOM^{Cre}* mice with AAV DIO ChR2-mCherry, and wild-type and *GAD67^{EGFP}* mice with AAV CaMKIIa.hChR2(h134a)mCherry.

Animals were anesthetized with isoflurane, mounted in a stereotactic apparatus and kept under isoflurane anesthesia during surgery. Injections were performed as described above. 150 nl of recombinant virus were injected in MEC or MS. We did not analyze mice in which the injection site did not correspond to the aimed area. Immunohistochemical and electrophysiological experiments were done 2-3 weeks after the treatments.

Immunohistochemistry

Mice were transcardially perfused with 4% paraformaldehyde (PFA). Sagittal sections (from MEC) or coronal sections (from MS) were cut at 40 µm thicknesses on a vibratome and washed with phosphate buffered saline (PBS). Free-floating sections were permeabilized and blocked for 2 hrs with PBS containing 5% BSA and 0.2% Triton X-100. The incubation of the sections with primary antibodies was performed for 24 hrs at 4°C. For double-labeling experiments both primary antibodies were incubated at the same time. Sections were washed with PBS and incubated for 2 hrs with Cy3-conjugated secondary antibody (1:1000 Jackson Immunoresearch,

Newmarket, UK) or AlexaFluor488 and Alexa647 secondary antibodies (1:1000; Invitrogen Darmstadt, Germany). After repeated washing with PBS the sections were mounted on 0.1% gelatin-coated glass slides and mounted in Mowiol 40-88. The sections were analyzed by confocal microscopy (Zeiss LSM 700).

Antibodies: Monoclonal anti-calbindin (1:5000, Swant, Bellinzona, Switzerland); polyclonal anti-calbindin (1:5000, Swant, Bellinzona, Switzerland); polyclonal calretinin (1:1000, Swant, Switzerland); polyclonal chicken EGFP (1:1000, Abcam, UK); monoclonal anti-NeuN (1:2000, Millipore, Temecula, CA, USA); monoclonal anti-parvalbumin (1:3000, Millipore, Temecula, CA, USA); monoclonal anti-reelin (1:1000, Millipore, Temecula, CA, USA), polyclonal rat somatostatin (1:1000, Millipore, Temecula, CA); monoclonal anti-VGAT (1:1000, Synaptic Systems, Goettingen, Germany); polyclonal WFS-1 (1:500, Proteintech Group, Inc. Chicago, IL, USA).

Image analysis

Anatomically matched sections were selected, spanning the lateral-medial extent of the MEC or the rostro-caudal extent of the MS. Confocal images were taken using a Zeiss LSM 700 microscope (Zeiss, Jena, Germany). Every third of 40 µm thick sagittal (MEC) or coronal (MS) sections were processed (each 120 µm apart) for each antibody to ensure complete analysis of each cell type across the analyzed brain area.

For quantification of retrogradely labeled neurons, three fields from the medial entorhinal cortex or medial septum (spanning the dorsal-lateral extent

of the section) for each brain section were taken with a 20× objective from a confocal microscope (Zeiss LSM 700). We analyzed seven sections from each animal. Data are presented as mean ± SEM.

Electrophysiology

Slice preparation

Electrophysiological recordings were performed from 6 to 12 weeks old mice. We recorded from acute sagittal slices (300 µm) containing dorsal MEC. The entorhinal and septal injection sites were controlled in horizontal and coronal sections, respectively. Mice were deeply anaesthetized with inhaled isoflurane, followed by transcardially perfusion with ~30 ml ice-cold sucrose solution containing (in mM) 212 sucrose, 26 $NaHCO_3$, 1.25 NaH_2PO_4, 3 KCl, 7 $MgCl_2$, 10 glucose and 0.2 $CaCl_2$, oxygenated with carbogen gas (95% O_2/ 5% CO_2, pH 7.4). Sections were cut in ice-cold oxygenated sucrose solution, followed by incubation in oxygenated extracellular solution containing (in mM) 12.5 NaCl, 2.5 $NaHCO_3$, 0.125 NaH_2PO_4, 0.25 KCl, 2 $CaCl_2$, 1 $MgCl_2$ and 25 glucose. Individual slices were placed in a submerged recording chamber mounted on an upright microscope (Olympus BW-X51) and continuously perfused with oxygenated extracellular solution. Cells in MEC and MS were visualized with DIC optics and epifluorescence was used to detect mCherry fluorescence.

Whole-cell recordings

Whole-cell patch-clamp recordings were performed at 30 to 32°C bath temperature. Recording pipettes were pulled from borosilicate glass

capillaries and had tip resistances of 3-8 MΩ. Liquid junction potentials were not corrected**.** Series resistance was maximally compensated and continuously monitored during the recordings. Cells were discarded if no "Giga seal" was initially obtained or series resistance changed more than 20% or was higher than 40 MΩ. The following intracellular solutions were used: low Cl^- potassium-based solution containing (in mM) 130 K-gluconate, 10 Na-gluconate, 10 Hepes, 10 phosphocreatine, 4 NaCl, 4 Mg-ATP and 0.3 GTP, pH adjusted to 7.2 with KOH. High Cl^- solution containing (in mM) 127.5 KCl, 11 EGTA, 10 Hepes, 1 $CaCl_2$, 2 $MgCl_2$ and 2 Mg-ATP (pH 7.3). Cs^+-based solution containing (in mM) 120 Cs^+-gluconate, 10 CsCl, 10 Hepes, 0.2 EGTA, 8 NaCl, 10 phosphocreatine, 2 Mg-ATP and 0.3 GTP, pH 7.3 adjusted with CsOH. For subsequent morphological and immunocytochemical characterization of patched cells, biocytin (circa 10 mg/ ml; Sigma) was added to the respective intracellular solution.

For paired recordings, layer II cells (from 83 mice) were visually identified and pairs of neurons whose somata were located at a distance of less than 40 µm were patched with low Cl^- potassium-based intracellular solution.

Cells were initially kept in cell-attached mode. After achieving a "Giga seal", whole-cell configuration was established and firing patterns were analyzed in current-clamp mode at resting membrane potential by applying 1 s current pulses, starting from -200 pA in 20 pA steps until maximal firing frequency was reached. Individual traces upon -200 pA current injection, at action potential threshold (for intermediate excitatory cell types) and upon 100 to 600 pA current injection (depending on cell type) were selected for illustration of firing pattern.

Classification of excitatory and inhibitory cells was done based on different electrophysiological parameters reported by others previously (Alonso and Klink, 1993; Couey et al., 2013; Lee et al., 2010). Electrophysiological parameters for excitatory cells are summarized in **Table S1.**

Interneurons were classified according to their typical firing pattern, with PV^+ FS interneurons exhibiting non-adapting firing of action potentials at > 80 Hz, in response to a 600 pA current step, while SOM^+ interneurons displayed a prominent hyperpolarizing sag, low-threshold firing (already at 60 pA current injection) and spike adaptation. The group of 5-HT_{3A}^{EGFP+} interneurons is diverse, consisting of at least 4 distinct interneuron subpopulations in MEC LII. The distinct interneuron subpopulations were identified according to their firing pattern and categorized as previously described by Lee et al. (Lee et al., 2010).

Putative connections were tested with 40 Hz trains (10 pulses) by injection of positive current (800 pA; 1-4 ms; in 10 s intervals) to elicit presynaptic action potentials, while postsynaptic cells were voltage-clamped either at -70 mV to detect uEPSCs or at -50 mV to obtain uIPSCs.

For analysis of possible connections and detection of even small response amplitudes an average of 25 sweeps was used and only stimulus-induced PSCs with a latency of less than 2.4 ms were considered as direct connections. A signal was considered positive only if the signal-to-noise ratio was higher than two. The excitatory connectivity was always verified by using the $GABA_A$ receptor antagonist Gabazine (10 µM; SR 95531 hydrobromide) followed by the AMPA receptor inhibitor CNQX (10 µM), whereas only CNQX had an effect on uEPSCs. Inhibitory connectivity was verified by bath

application of Gabazine, while a previous administration of CNQX (10 μM) did not affected uIPSCs.

For long-range MEC-MEC connection experiments, target cells (from 39 mice) were characterized according to their firing properties in current-clamp configuration as described above. Traces upon -200 pA current injection, at action potential threshold and, in the case of FS interneurons at maximal firing frequency, were selected for illustration of firing pattern. Synaptic inputs were analyzed at a holding potential of -70 mV. EPSCs were recorded in response to 5 ms laser-stimulations (473 nm) using approximately 120 mW/mm^2 laser power. Individual synaptic inputs were tested using the following pharmacological agents: CNQX (10 μM), D-AP5 (50 μM), Gabazine (10 μM), TTX (1 μM) and 4-AP (100 μM), bath-applied.

For septal-MEC connection experiments, cells were patched with high Cl^- intracellular solution and classified based on their firing patterns in current-clamp mode (see MEC-MEC experiments; for illustrations of firing patterns traces upon -50 pA current injection, at AP threshold and maximal firing frequency were selected). Cells were voltage-clamped at -80 mV to analyze PSCs induced by laser-stimulation. In some experiments, cells were first classified with K^+-based intracellular solution and then repatched with Cs^+-based solution to analyze the reversal potential. To test the effect of laser-stimulation onto spontaneous firing, identified targeted fast-spiking cells were patched with K^+-based solution. In these cases, cells were depolarized to suprathreshold potentials in current clamp mode and 31 to 232 sweeps of 3 s duration each were recorded. In the middle of each sweep, long-range projections were stimulated for 1s with 8 Hz laser pulses of 60 ms duration.

All recordings were made using either HEKA PatchMaster EPC 8 or 10 amplifier and signals were filtered at 3 kHz, sampled at 10 or 20 kHz. Data analysis was done offline using HEKA software FitMaster or MatLab (Mathworks). Data are given as mean ± SEM. P-values were calculated with Student's t-test, repeated measures ANOVA and Tukey HSD test in Excel (Microsoft) and SPSS (Version 12.0.1 for Windows). Normal distribution of data was tested with the Kolmogorov-Smirnov test.

Cell identification and reconstruction

Acute slices with biocytin-filled cells in the MEC were fixed overnight in 4% paraformaldehyde, followed by extensive washing with PBS.

For immunocytochemical analysis, acute slices were resliced into 60 µm sections and biocytin-labeling was visualized using streptavidin-Cy3 or streptavidin-Cy2 (both 1:1000, Life Technologies GmBH, Frankfurt, Germany). Subsequent stainings against PV, RE, WFS1 and calretinin were conducted as described in the immunohistochemical section.

For morphological reconstructions, biocytin-filled MEC cells were identified via 3,3'-diaminbenzidine (DAB) staining. Sections were fixed overnight in 4% paraformaldehyde, washed and quenched in 1% H_2O_2 for 5 min. After renewed washing, sections were permeabilized in PBS with 1% Triton X-100 for 1 hr. Subsequently, sections were incubated with avidin-biotin-horseradishperoxidase complex in PBS for 2 hrs at room temperature. Following washing in PBS, sections were developed in DAB and mounted in Mowiol. Labeled cells were reconstructed using the Neurolucida (MBF bioscience, Willston, VT, USA) tracing program. Morphological and Sholl

analysis of reconstructed cells have been performed using Neurotrace (MBF bioscience, Willston, VT, USA). Data are given as mean ± SEM. P-values were calculated with repeated measures ANOVA and Bonferroni post-hoc test using Prism (GraphPad Software, La Jolla, Ca, USA).

A principal component analysis based on the variables sag, spike latency, ISI1/2, dAP and the presence of an apical dendrite was conducted in R (software R version 3.01 and using the function “princomp”). For this purpose all variables were normalized to a standard deviation of 1.

Supplemental References

Alonso, A., and Klink, R. (1993). Differential electroresponsiveness of stellate and pyramidal-like cells of medial entorhinal cortex layer II. J.Neurophysiol. 70, 128-143.

Cardin, J.A., Carlen, M., Meletis, K., Knoblich, U., Zhang, F., Deisseroth, K., Tsai, L.H., and Moore, C.I. (2010). Targeted optogenetic stimulation and recording of neurons in vivo using cell-type-specific expression of Channelrhodopsin-2. Nat. Protocols 5, 247-254.

Couey, J.J., Witoelar, A., Zhang, S.J., Zheng, K., Ye, J., Dunn, B., Czajkowski, R., Moser, M.B., Moser, E.I., Roudi, Y., and Witter, M.P. (2013). Recurrent inhibitory circuitry as a mechanism for grid formation. Nat. Neurosci. 16, 318-324.

Hippenmeyer, S., Vrieseling, E., Sigrist, M., Portmann, T., Laengle, C., Ladle, D.R., and Arber, S. (2005). A developmental switch in the response of DRG neurons to ETS transcription factor signaling. PLoS Biol. 3, e159.

Inta, D., Alfonso, J., von Engelhardt, J., Kreuzberg, M.M., Meyer, A.H., van Hooft, J.A., and Monyer, H. (2008). Neurogenesis and widespread forebrain migration of distinct GABAergic neurons from the postnatal subventricular zone. Proc. Natl. Acad. Sci. U S A 105, 20994-20999.

Klugmann, M., Symes, C.W., Leichtlein, C.B., Klaussner, B.K., Dunning, J., Fong, D., Young, D., and During, M.J. (2005). AAV-mediated hippocampal expression of short and long Homer 1 proteins differentially affect cognition and seizure activity in adult rats. Mol. Cell. Neurosci. 28, 347-360.

Lee, S., Hjerling-Leffler, J., Zagha, E., Fishell, G., and Rudy, B. (2010). The largest group of superficial neocortical GABAergic interneurons expresses ionotropic serotonin receptors. J. Neurosci. 30, 16796-16808.

Melzer, S., Michael, M., Caputi, A., Eliava, M., Fuchs, E.C., Whittington, M.A., and Monyer, H. (2012). Long-range-projecting GABAergic neurons modulate inhibition in hippocampus and entorhinal cortex. Science 335, 1506-1510.

Tamamaki, N., Yanagawa, Y., Tomioka, R., Miyazaki, J.I., Obata, K., and Kaneko, T. (2003). Green fluorescent protein expression and colocalization with calretinin, parvalbumin, and somatostatin in the GAD67-GFP knock-in mouse. J. Comp. Neurol. 467, 60-79.